Synthesis and Properties of Epoxies Containing Rigid Rods in the Side Chains

K. H. Hsieh,[1] S. B. Ji,[1] H. R. Wang,[1] G. H. Ho,[1] J. L. Han[2]

[1]*Department of Chemical Engineering, Institute of Polymer Science and Engineering, National Taiwan University, Taipei, Taiwan 106*
[2]*Department of Chemical and Materials Engineering, National I-Lan University, I-Lan, Taiwan 260*

Received 19 October 2004; accepted 26 May 2005
DOI 10.1002/app.23108
Published online in Wiley InterScience (www.interscience.wiley.com).

ABSTRACT: A novel epoxy containing rigid rods in the side chain (SR-epoxy) was synthesized by bulk polymerization. The SR-epoxy resins were characterized by Fourier transform infrared. The cured SR-epoxies showed excellent mechanical properties and high thermal stabilities. Scanning electron microscopy (SEM) of the cured SR-epoxy illustrated a fiber-like morphology. The thermal properties, dynamic mechanical properties, compatibility, and morphology of the SR-epoxies were extensively investigated in the study. SEM photographs showed that there were some fiber-like structures in the system of the SR-epoxy containing the rigid-rod group 4,4′-bis(6-hydroxyhexoxy) biphenyl, which formed a self-reinforcing composite. © 2006 Wiley Periodicals, Inc. J Appl Polym Sci 101: 4030–4036, 2006

Key words: reinforcement; scanning electron microscopy (SEM); structure

INTRODUCTION

Liquid-crystalline polymers (LCPs) are new and high-performance engineering plastics. They possess unique mechanical and processing properties. As such, they are becoming noticeable in material engineering. More and more applications of LCPs have been found recently. The current trend is toward LCPs as composite reinforcements or as matrices. The use of the rigid rod structure of LCPs to reinforce flexible polymers as molecular composites is another new field.[1–5]

As is well known, one great feature of LCPs is their anisotropic properties. Because of their stiff rod-like structure, they can reinforce the matrix as the fiber does. If one can control the degree of LCP orientation in the matrix, the mechanical properties will be under control. Compared to ordinary composites, molecular composites have decreased disadvantages of interfacial contact, phase separation, and fiber defects. Consequently, these composites possess much better reinforcement effects. Research and development on the use of LCPs as a blend ingredient, compatible agent, or liquid-crystalline elastomer have largely improved the mechanical properties, dimensional stability, and processing viscosity. LCP composites have been shown to have better compatibility than fiber-reinforced composites.

Epoxy is a kind of "magic" resin.[6–10] It can adhere to metals, wood, glass, and ceramics very well. Epoxy features include easy processing, low shrinkage, excellent mechanical properties, good thermal stability, good chemical resistance, and good electrical insulation. So it is usually used as the matrix of a composite. It possesses a very important position in the field of composites.

In this study, we aimed to modify the side chain of epoxy resin to synthesize a self-reinforcing composite by introducing a little bit of a liquid-crystalline source.

EXPERIMENTAL

The materials used and their designations are listed in Table I.

Preparation of the mesogenic group 4,4′-bis(6-hydroxyhexoxy) biphenyl (BHHBP)[1–5]

BHHBP was prepared as follows: sodium hydroxide (32.00 g, 0.800 mol) and 4,4′-dihydroxybiphenyl (37.2 g, 0.200 mol) were stirred into 400 mL of ethanol. The resulting slurry was heated under reflux, and 6-chloro-1-hexanol (120.2 g, 0.880 mol) was added dropwise. The reaction mixture was refluxed for 24 h

Correspondence to: K. H. Hsieh (khhsieh@ntu.edu.tw).
Contract grant sponsor: National Science Council, Taipei, Taiwan; contract grant number: NSC89-2216-E-197-003.
Contract grant sponsor: Ministry of Economic Affairs, Taipei, Taiwan; contract grant number: 91-EC-17-A-08-S1-0015.

TABLE I
Materials

Designation	Description	Source
BP	4,4′-Biphenol	ACROS
NaOH	Sodium hydroxide	ACROS
EtOH	Ethanol	ACROS
6-Chloro-1-hexanol	6-Chloro-1-hexanol	TCI Chemical, Japan
MDI	4,4′-Diphenyl methane diisocyanate	BASF Wyandotte Co., Switzerland
DGEBA (DER331)	Diglycidyl ether of biphenol A, EEW = 186	Dow Chemical Co.
TDMP	2,4,6-Tri(dimethyl aminomethyl) phenol	Ciga-Geigy Co., Switzerland

and then poured into cold water. The reaction is shown in Scheme 1.

The precipitated solid was filtered and recrystallized to produce BHHBP (mp = 166–172°C).

Preparation of epoxies containing rigid rods in the side chains (SR-epoxies)

First, the NCO-terminated pendent hydroxyl group of the epoxy prepolymer was synthesized by a variable equivalent ratio of epoxy (DER331) and 4,4′-diphenyl methane diisocyanate (MDI) under a nitrogen atmosphere at a temperature of approximately 80°C in a four-necked flask with a mechanical stirrer. During the reaction, samples were drawn for IR analysis. The reaction was curtailed when the —NCO peak (2270 cm^{-1}) decreased to half of its initial value. It was the pendant hydroxyl group on the epoxy that fully reacted with one end of the isocyanate group on MDI. Second, a suitable amount of BHHBP was added into the flask, and then, the temperature was increased to 105°C. After several hours, samples were drawn for Fourier transform infrared (FTIR) analysis. The reaction was curtailed until the —NCO peak disappeared, which ensured that the hydroxyl group on BHHBP was fully reacted with the isocyanate group on MDI. As to the curing of the SR-epoxy, a suitable amount of the previous SR-epoxy was placed in a cup, into which 3 phr curing agent [2,4,6-tri(dimethyl aminomethyl) phenol (TDMP)] was added; and then, they were vigorously stirred. The reaction mixture was poured into an aluminum mold and pressed at 120°C for 1 h. The sample was then postcured at 150°C for 2 h. The sample was removed from the mold and placed on a desiccator, where the relative humidity was maintained at 50% for 3 days before testing.

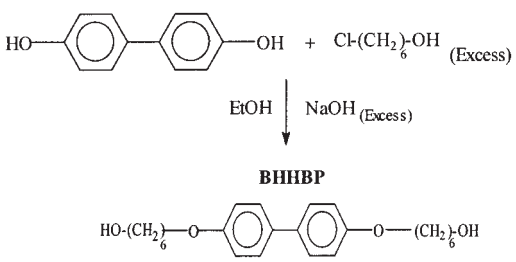

Scheme 1

Testing method

FTIR analysis was performed on a Bio-Rad FTS-40 FTIR spectrophotometer at a 4-cm^{-1} resolution. We directly applied the samples by dabbing them onto KBr pellets. The rheological data was measured with a viscometer (Brook-Field model LVDVII+). Testing was performed at a fixed shear rate of 100 rpm over a temperature range of 40–150°C.

The stress–strain properties were measured with a tensile testing instrument (Yashima Works, Ltd., Co., Japan, model RTM-IT). The stress–strain test procedure was followed as described in ASTM D 638 with a crosshead speed of 10 mm/min; at least five specimens were used for the test. The fracture energy (G_{IC}) test procedure was followed as described for compact tension specimens.[11] A sharp precrack was made with a razor blade before the test. The specimens were tested on a screw-driven Instron machine at a crosshead speed of 1 mm/min. The Izod impact strength test was performed on a Toyo Seiki-Sho., Ltd., instrument (model CH-1679) with a hammer of 40 kgf. The test was followed as described in ASTM D 256, with a notch at 45°C. The sample size was approximately 63 × 12.7 × 6 mm, and at least five specimens were used for the test.

Differential scanning calorimetry (DSC) analysis was performed on a DuPont 2010 instrument at a heating rate of 20°C/min for crosslinked polymers over a temperature range of −100 to 250°C. The glass-transition temperature (T_g) was determined at the midpoint of the transition in heat capacity. Thermogravimetric analysis (TGA) of the crosslinked polymer samples were carried out on a PerkinElmer TGA-7 in a nitrogen atmosphere. The measurements were performed at a heating rate of 10°C/min over a temperature range from 40 to 800°C. The weight of the samples tested was about 8 mg. Dynamic mechanical analysis (DMA) was performed on a PerkinElmer DMA-7 over a temperature range from −120 to 300°C. The

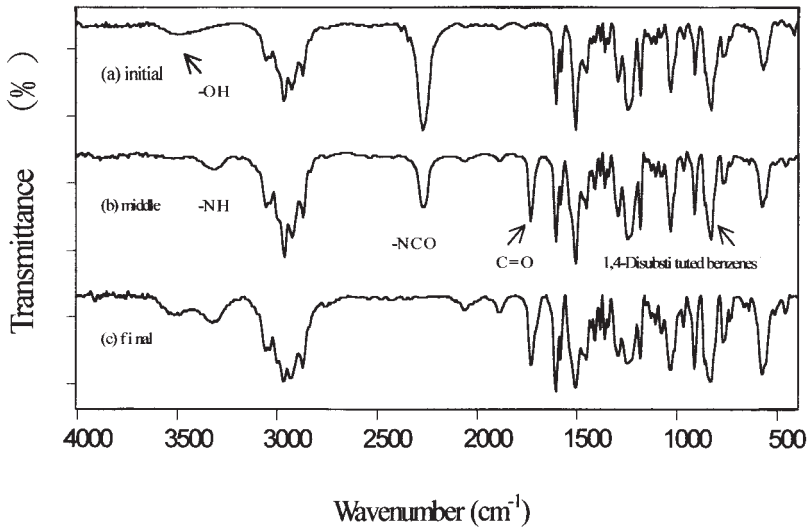

Figure 1 FTIR spectra during the SR-epoxy reaction: (a) initial; (b) middle; (c) final.

heating rate was set at 5°C/min. The sample size was approximately 2 × 10 × 20 mm.

Morphological studies were performed with scanning electron microscopy (SEM). The samples were dipped in liquid nitrogen and cut into sections. A Jeol JSM-6300 scanning electron microscope was used for the morphology observations.

RESULTS AND DISCUSSION

FTIR analysis

The reaction between the epoxy (DER331) and MDI mixture is shown in Figure 1. The intensity of the characteristic peak of the isocyanate group (—NCO, 2270 cm^{-1}) gradually decreased with as the reaction proceeded. When the intensity of the characteristic peak of isocyanate (—NCO, 2270 cm^{-1}) decreased to half of its initial value, the BHHBP was added. The reaction was finished when the characteristic peaks of the isocyanate group disappeared and the characteristics of the carbonyl group (—OH, 3500 cm^{-1}) appeared, as shown in Figure 1(c). SR-epoxy was formed.

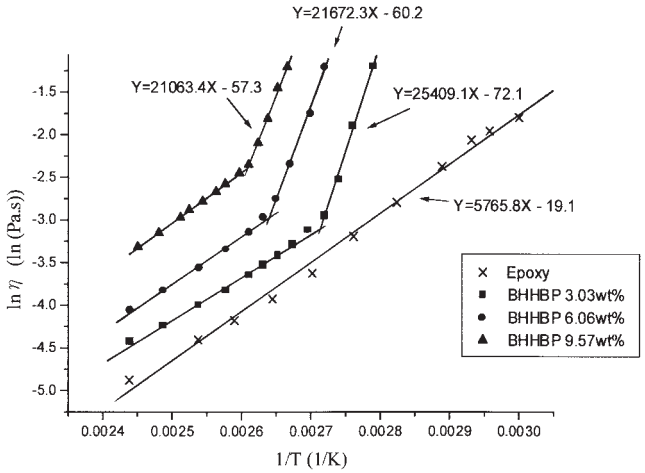

Figure 2 E_a of values of the SR-epoxies with various BHHBP contents.

Rheological analysis

The viscosity of LCP obviously changed during the phase-transition temperature because of the rod-like structure. There are many viscoelastic properties and molecular motions that are different between rod-containing polymers and ordinary polymers.[12] With the WLF equation, one can derive the flow activation energy at a constant shear strain rate (E_a), as shown in eq. (1):

$$\eta = f(\text{Shear strain rate}, T)$$

$$\eta = A \exp(E_a/RT), \text{ Fixed shear strain rate constant}$$

$$\ln \eta = E_a/RT + \ln A \quad (1)$$

TABLE II
E_a Values of the Neat Epoxy and SR-Epoxies

Composition	E_{a1} (cal/gmol K)	E_{a2} (cal/gmol K)
Neat epoxy	—	11,456.64
3.03 wt % BHHBP	50,487.88	10,004.74
6.06 wt % BHHBP	43,062.86	10,985.73
9.57 wt % BHHBP	41,852.98	11,794.63

E_a = Slope of line × 1.987 (cal/gmol K).

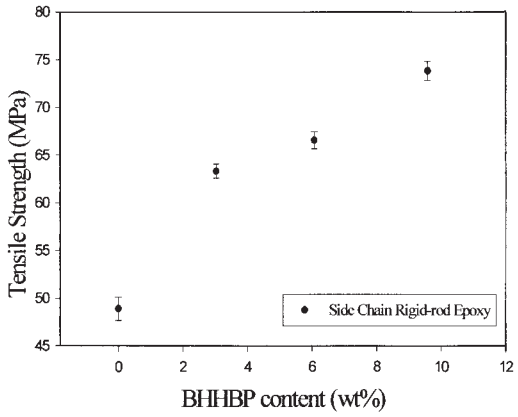

Figure 3 Tensile strengths of the SR-epoxies with various BHHBP contents.

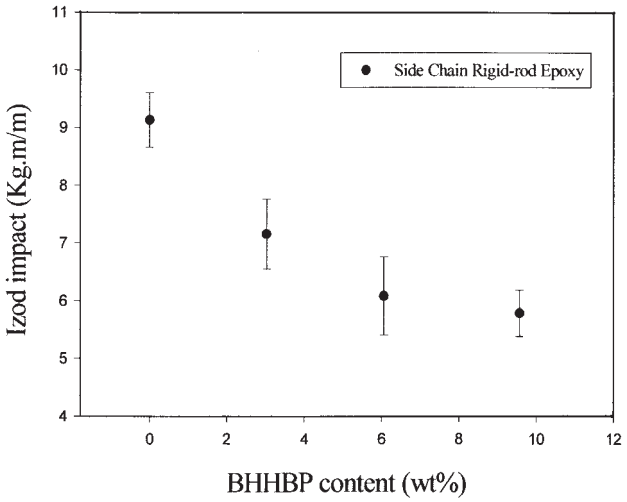

Figure 4 Izod impact strengths of the SR-epoxies with various BHHBP contents.

where η is the apparent viscosity, T is the temperature, R is the ideal gas constant, and A is a constant.

The flow activation energies of the low-temperature and high-temperature regions were E_{a1} and E_{a2}, respectively. As shown in Figure 2, at a fixed shear rate, there were two E_a's (E_{a1} and E_{a2}) in the SR-epoxy system regardless of the variation in BHHBP content. This was consistent with the properties of LCPs; the viscosity changed dramatically during the phase transition of LCP. The rheological properties of the newly developed SR-epoxy were the same as the LCP. A phase transition existed in this system. As shown in Table II, E_{a1} decreased increasing BHHBP content. In the low-temperature region, the side chain molecule motion dominated E_{a1}. The increase in BHHBP content increased the degree of orientation. Therefore, E_{a1} decreased with increasing BHHBP content. In the high-temperature region, the epoxy matrix dominated E_{a2}, although the BHHBP was introduced. E_a of the SR-epoxy was close to that of the neat epoxy resin in the high-temperature region.

Stress–strain properties

Figure 3 shows the relation between the tensile strength of the SR-epoxies and the BHHBP content. Figure 3 shows the trend of increasing tensile strength with increasing BHHBP content. The BHHBP molecule was a rigid rod-like structure. So, the tensile strength increased because the rigid rod-like structure in the SR-epoxies had bearing on the effect of reinforcement. With the introduction of the small rigid-rod group BHHBP, the increase in tensile strength was remarkable. The results are listed in Table III.

Fracture toughness

Izod impact strength is a kind of high-shear-rate fracture behavior. Figure 4 shows the relation between the Izod impact strength of the SR-epoxies and the BHHBP content. Epoxy is a kind of brittle material. After the rigid-rod group BHHBP (rod-like structure) was introduced, the epoxy resin became less tough. This was due to the existence of dangling chains (BHHBP group), which decreased the crosslink density. Therefore, when under high-shear-rate fracture (Izod impact strength), the SR-epoxy was easily fractured. The Izod impact strength decreased with increasing BHHBP content, as shown in Table III.

Figure 5 shows the relation between G_{IC} of the SR-epoxies and the BHHBP content. With increasing BHHBP content, the G_{IC} value of SR-epoxy shifted upward. After the rigid-rod group BHHBP was introduced into the SR-epoxy system, it had a fiber-like heterogeneous morphology, as clearly observed in the

TABLE III
Mechanical Properties of the SR-Epoxies

Mechanical property	BHHBP content (SR-epoxy)			
	0 wt %	3.03 wt %	6.06 wt %	9.57 wt %
Tensile strength (Mpa)	48.9	63.3	66.5	73.8
Izod impact strength (Kgf m/m)	9.1	7.2	6.1	5.7
G_{IC} (kJ/m^2)	5.2	21.3	24.1	26.0

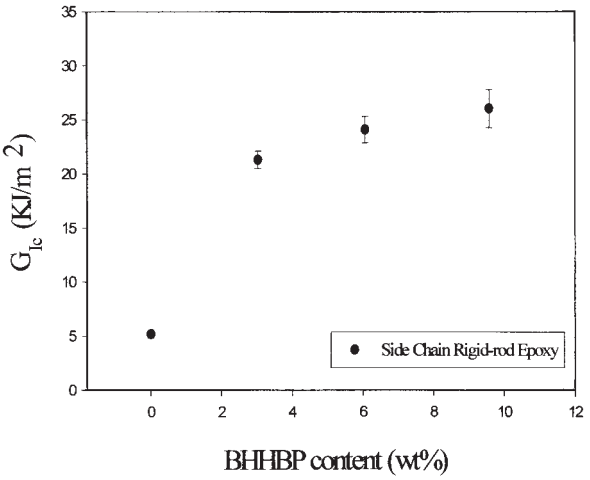

Figure 5 G_{IC} values of the SR-epoxies with various BHHBP contents.

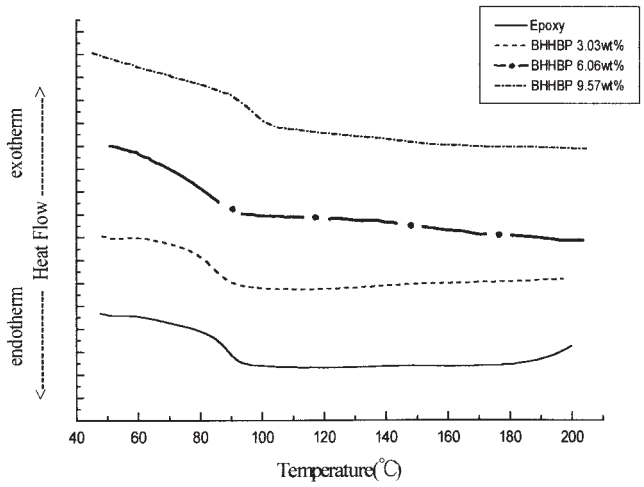

Figure 7 DSC graph of the SR-epoxies with various BHHBP contents.

SEM graph (Fig. 10, shown later). G_{IC} is a kind of low-shear-rate fracture behavior, so it closely depends on the morphology of the sample. The rigid-rod group in this system acted as a short-fiber reinforcing this system. Therefore, G_{IC} of the SR-epoxy increased with increasing BHHBP content, as shown in Table III.

Thermal analysis

Figure 6 shows the DSC graph of the pure mesogenic group BHHBP. There were two distinct endothermic peaks during heating and exothermic peaks during cooling. They were melting temperature (T_m or T_c) and isotropic temperature (T_i), respectively. That means the BHHBP possessed liquid-crystalline behavior. In the heating stage (10°C/min), the transition temperature between the liquid-crystalline domain and crystalline domain (or mesophase) was 93.3°C. The transition temperature between the liquid and liquid-crystalline domains was 172.3°C. In the cooling stage (10°C/min), the transition temperature between the liquid and liquid-crystalline domains was 166.4°C. The transition temperature between the crystalline domain and the liquid-crystalline domain was 80.7°C. These results corresponded with those of previous studies.[2,3]

Figure 7 shows the DSC graph of the cured SR-epoxies. With increasing BHHBP content, T_g decreased and then increased. Because of the side chain effect, the alignment of the molecular chain became more compact, and the free volume of the molecular segment increased. So T_g decreased when the rigid-rod group content increased. T_g increased when the rigid-rod group BHHBP content was up to 9.57%, because the rigid-rod structure of BHHBP contributed to the alignment of the molecular chains.

Figure 8 shows the TGA graph of the SR-epoxy resins with various BHHBP contents. The testing was done under inert conditions. The main purpose was to

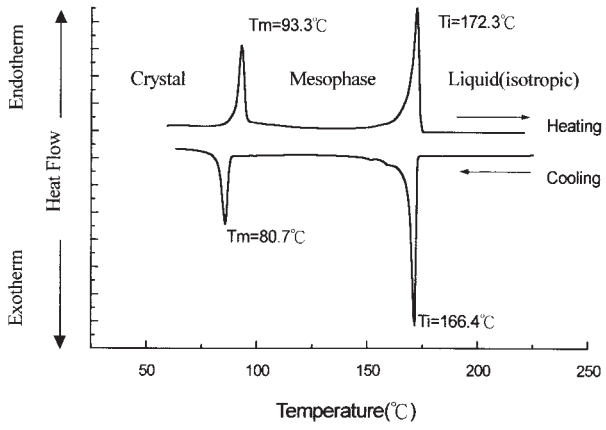

Figure 6 DSC graph of pure BHHBP.

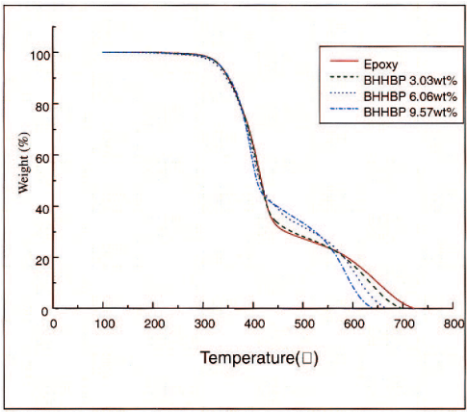

Figure 8 TGA graph of the SR-epoxies with various BHHBP contents. [Color figure can be viewed in the online issue, which is available at www.interscience.wiley.com.]

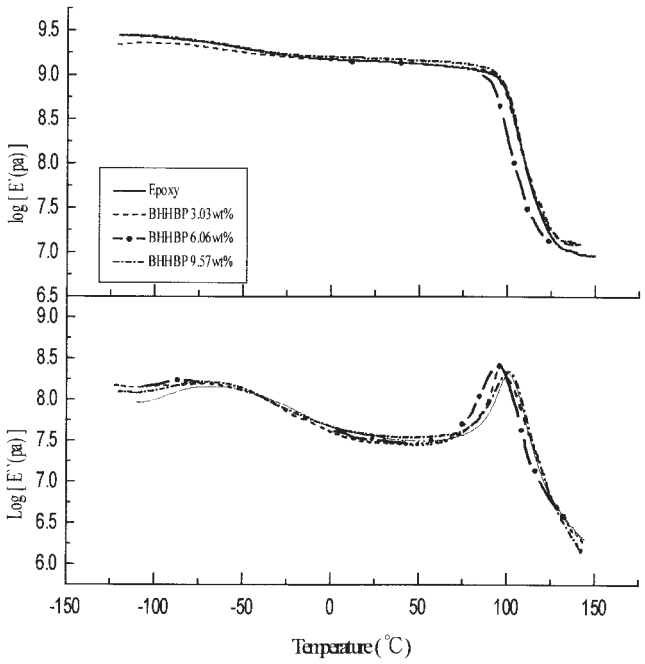

Figure 9 DMA graph of the SR-epoxies with various BHHBP contents.

measure the thermal decomposition temperature and char yield. The BHHBP content did not affect the thermal decomposition temperature. However, that means the thermal stability in the SR-epoxy system was as good as that in the neat epoxy system.

DMA

There were two distinct peaks in the DMA figure of the pure epoxy; one in the low-temperature transition region (T_{gl}, β-transition), which was about -60°C, and the other in the high-temperature transition region (T_{gh}, α-transition), which was about 100°C. In the neat epoxy resin, they represented the molecular motions of the hard segment of the main chain and the molecular motions of the soft segment of the main chain, respectively. Figure 9 shows that with increasing rigid-rod group BHHBP content, T_{gl} and T_{gh} were on the downside first and then rose. Because of the SR-epoxy system, the alignment of molecules became less close. The main chain had less molecular motion, so

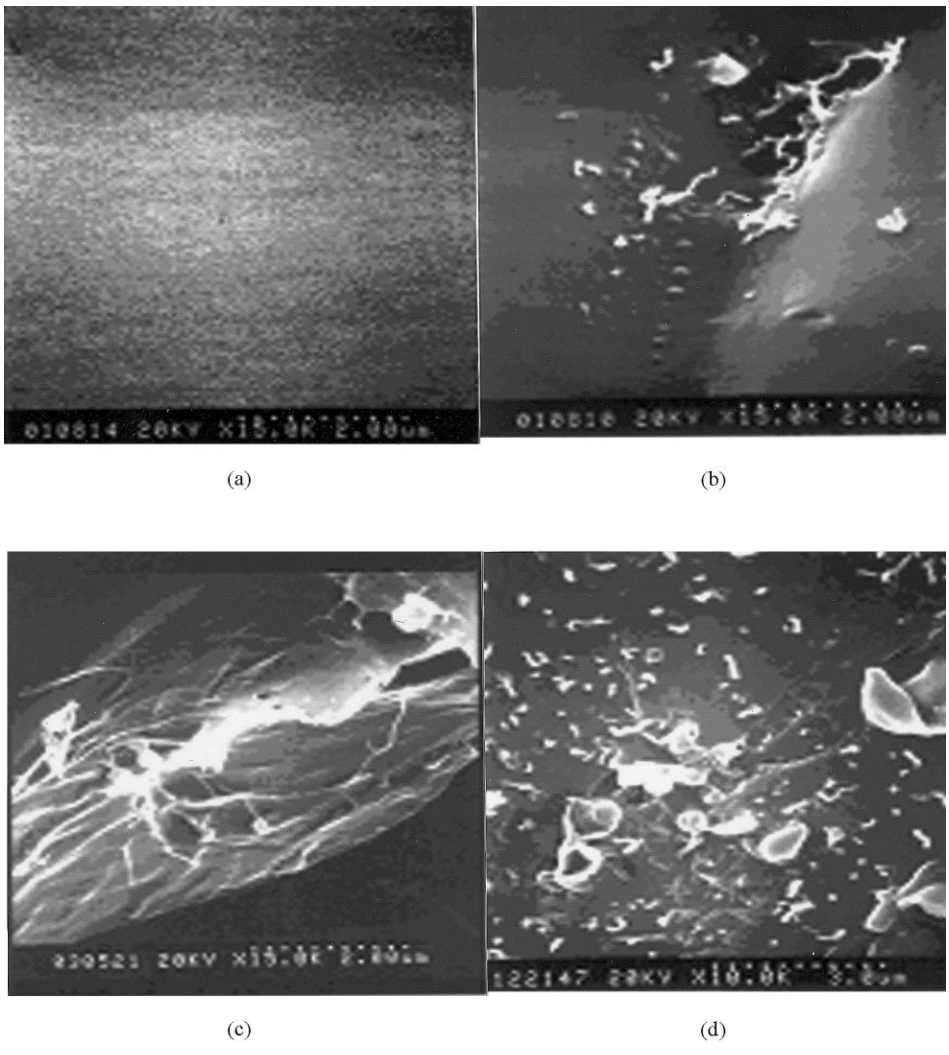

(a) (b)

(c) (d)

Figure 10 SEM photographs for the SR-epoxies with various BHHBP contents: (a) 0, (b) 3.03, (c) 6.06, and (d) 9.57 wt %.

T_{gh} decreased with the 3.03 and 6.6 wt % BHHBP contents. However, when the BHHBP content continuously increased, T_{gh} increased. It was apparent that the increase in the rigid-rod group BHHBP content increased the alignment of the molecular chains. The motion of the main chain became less flexible. Also, T_{gl} behaved as well as T_{gh}. This meant that the molecular motions of the soft-segment region became much more ordered when the BHHBP content was increased to a certain extent. So T_{gl} tended to go upward.

Morphology

Figure 10 shows the SEM graphs of the microstructures in the SR-epoxies. A fiber-like structure was found in the SR-epoxies in the SEM graphs when the rigid-rod group BHHBP was introduced. With increasing BHHBP content, the fiber-like structure became more evident. The fiber-like structure in the system could produce the self-reinforcement effect. From the results, we concluded that the rigid rods in the side chain were beneficial for the wiggle and aggregation between molecules. So some fiber-like structures appeared in the epoxy matrix.

CONCLUSIONS

The tensile strength of the SR-epoxy was higher than the neat epoxy because there were some fiber-like structures in the SR-epoxy system. The rigid rod-like structure produced the self-reinforcement effect. In the SR-epoxy system, G_{IC} increased with increasing BHHBP content. As shown in the DSC graph, T_g of the SR-epoxies was on the downside first and then rose with increasing BHHBP content. In the SR-epoxy system, the DSC analyses results were consistent with the DMA results. The SEM graphs showed that the introduction of the rigid-rod group into the epoxy matrix produced a fiber-like structure. It produced a self-reinforcement effect. Therefore, the SR-epoxy showed excellent tensile and G_{IC} properties.

References

1. Stenhouse, P. J.; Valles, E. M.; Kantor, S. W.; Macknight, W. J. Macromolecules 1989, 22, 1467.
2. Smyth, G.; Pollack, S. K.; Macknight, W. J.; Hsu, S. L. Liq Cryst 1990, 7, 839.
3. Khan, N.; Patel, V. L.; Bashir, Z.; Price, D. M. J Polym Sci Part B: Polym Phys 1995, 33, 1957.
4. Bashir, Z.; Khan, N. J Polym Sci Part B: Polym Phys 1996, 34, 2077.
5. Reck, B.; Ringsdorf, H. Makromol Chem Rapid Commun 1985, 6, 291.
6. Lee, H.; Neville, K. Handbook of Epoxy Resin; McGraw-Hill: New York, 1967.
7. Hsieh, K. H.; Han, J. L. J Polym Sci Part B: Polym Phys 1990, 28, 623.
8. Hsieh, K. H.; Han, J. L. J Polym Sci Part B: Polym Phys 1990, 28, 783.
9. Han, J. L.; Tseng, S. M.; Mai, J. H.; Hsieh, K. H. Angew Makromol Chem 1990, 182, 193.
10. Han, J. L.; Tseng, S. M.; Mai, J. H.; Hsieh, K. H. Angew Makromol Chem 1991, 184, 89.
11. Ting, R. Y.; Cottington, R. L. J Appl Polym Sci 1980, 25, 1815.
12. Ferry, J. D. Viscoelastic Properties of Polymers, 3rd ed.; Wiley: New York, 1980.